The Calibration Index and Taxonomy for Robot Kinematic Calibration Methods

John M. Hollerbach and Charles W. Wampler

The International Journal of Robotics Research 1996; 15; 573
DOI: 10.1177/027836499601500604

The Calibration Index and Taxonomy for Robot Kinematic Calibration Methods

John M. Hollerbach
Departments of Mechanical Engineering
and Biomedical Engineering
McGill University
Montreal, Quebec, Canada H3A 2B4

Charles W. Wampler
Mathematics Department
General Motors Research and Development
Warren, Michigan 48090

Abstract

The major approaches toward kinematic calibration are unified by considering an end-point measurement system as forming a joint and closing the kinematic loop. A calibration index is introduced, based on the mobility equation, that considers sensed and unsensed joints and single and multiple loops and expresses the surplus of measurements over degrees of freedom at each pose. Past work using open-loop calibration, closed-loop calibration, and screw axis measurement is classified according to this calibration index. Numerical issues are surveyed, including task variable scaling, parameter variable scaling, rank determination, pose selection, and input noise handling.

1. Introduction

Calibration is at the heart of experimental and autonomous robotics. For experimental robotics, without careful controls and calibration, the significance or veridicality of results cannot be gauged. We should expect to spend most of our experimental effort in calibration and relatively less in actually running the experiments in robot control (Hollerbach and Hunter 1990). For autonomous robotics, a robot will need to develop and periodically update its internal model for best performance. These intuitions may explain the considerable recent literature in robot calibration. Ideally, the calibration methods should be statistically robust, there should be a variety of approaches for different circumstances, and metrology equipment should be sufficiently accurate, convenient to use, and not too expensive. The robot should also be capable of calibrating itself with minimal human involvement.

The International Journal of Robotics Research,
Vol. 15, No. 6, December 1996, pp. 573–591,

J. M. Hollerbach is currently with the Department of Computer Science, University of Utah, Salt Lake City, Utah 84112.

This article focuses primarily on kinematic calibration methods. A large variety of methods have been proposed that differ according to measurement system (open-loop methods), passive end-point constraints (closed-loop methods), and pose organization (screw axis measurement methods):

1. *Open-loop methods.* The large majority of proposed methods require an external metrology system to measure the pose of an end effector. The number of measured pose components can vary from six (full pose) to just one component of pose. In open-loop methods, individual poses are attained by moving all the joints, and the kinematic parameters are found from a nonlinear optimization of the total pose set (Mooring et al. 1991).
2. *Closed-loop methods.* By attaching the end effector to the ground and forming a mobile closed kinematic chain, calibration is achieved using joint angle sensing only, without any external metrology system (Bennett and Hollerbach 1991). The end-point constraints may vary from full rigidity (six degrees of constraint) to only one motion constraint, and there may be multiple kinematic loops. Parameter estimation proceeds as for the open-loop methods.
3. *Screw-axis measurement methods.* These methods identify individual joint axes as lines in space. From this knowledge, the kinematic parameters can be found analytically without the numerical search requirements of the open- and closed-loop methods (Sklar 1989). In circle point analysis (CPA), poses are organized by moving the end point in a circle by one joint at a time and measuring its position (Stone 1987).

The distinctions among these methods are often small and arbitrary. For example, certain open-loop methods constrain some components of pose, as well as measure

others; this mixes aspects of open- and closed-loop methods. Furthermore, parallel mechanisms have mixtures of sensed and unsensed joints, and these unsensed joints are formally no different from passive task kinematics for closed-loop methods.

1.1. The Calibration Index

Given what is becoming a bewildering variety of kinematic calibration approaches, it is not always clear what is the relationship among such approaches and what are the advantages or disadvantages. It is a goal of this article to provide a unifying taxonomy as follows.

By viewing the external measurement system as forming a joint that closes the base with the end effector, all of the methods above can be considered as closed-loop methods (Wampler and Arai 1992; Wampler et al. 1995). In such closed loops, some of the joints may be sensed (due to joint angle sensors or measured components of pose), while other joints may be unsensed (due to unsensed joint angles, passive unsensed end-point constraints, or unmeasured components of pose).

Because everything is now a closed loop, one may therefore employ the mobility equation to determine the degrees of freedom of the resulting mechanism. If the number of joint sensors (including the measurement "joint") exceeds the mobility, then calibration is possible. The excess of sensing over mobility is termed the *calibration index,* which represents the number of independent equations per pose available for calibration. Previous methods can then be categorized and compared based on their calibration indices. This viewpoint is especially useful for multiple-loop calibration, where because of mechanism complexity it may be difficult to compare methods. This viewpoint also considers as equivalent a measurement of a pose component or a constraint of a pose component, thereby unifying open- and closed-loop methods, which are now termed *kinematic loop methods,* discussed in Section 2.

1.2. Numerical Issues

Numerical issues can critically affect the accuracy of calibration. These include task variable scaling, parameter variable scaling, rank determination, pose selection, and handling input noise. In particular, scaling issues are not often addressed in the calibration literature, while consideration of input noise is practically absent.

- Task variable scaling addresses differences in accuracies with which different components of pose are measured and in mixing units such as radians and meters in a least-squares objective function. The general solution is weighted least squares, particularizations of which include the Gauss-Markov estimate.
- Parameter variable scaling addresses (potentially vastly) different scales of the parameters, and what effect this might have on numerical conditioning. Solutions include column scaling and model-based scaling. Weighted a priori estimates of nominal parameter values can be incorporated into the objective function to yield damped least squares, a particularization of which is the minimum variance estimate, related to the Kalman filter.
- Rank determination addresses the identifiability of the desired kinematic parameters and is handled through singular value decomposition. One may proceed either by model reduction or by zeroing small singular values.
- Pose determination involves the selection of sufficient poses for robust identification by the use of various observability measures. A formal correspondence between proposed observability measures and redundancy resolution measures in a different area of robotics is drawn.
- Last, input noise (i.e., joint angle measurement noise) is often significant relative to output noise (i.e., end-point pose measurement noise). In fact, for the closed-loop methods there is practically no output noise (except for attachment backlash), and so it is inappropriate to minimize the output prediction error. It is well known that input noise leads to bias errors in estimation. The method to handle input noise is total least squares or orthogonal distance regression. An extension is the implicit loop method (Wampler et al. 1995), which is based on the viewpoint of all calibration methods as closed-loop methods (leading to an implicit constraint equation) and places all measurements (whether joint or end-point) on an equal footing.

1.3. Screw Axis Measurement

The last section reviews screw axis measurement methods, which determine the individual joint axes as lines in space.

- In CPA, single joints are moved at a time in a circle while a point on the end effector is measured. Recently, triaxial accelerometers have been employed instead of position sensors.
- In Jacobian measurement methods, the joint screws are all determined simultaneously by measuring the Jacobian matrix. The Jacobian matrix may be measured using either end-effector velocity sensing

plus joint velocity sensing, or end-effector wrench sensing plus joint torque sensing.

As opposed to the nonlinear parameter search in the kinematic loop methods, a recursive procedure can be employed to extract the parameters from the joint screws quite straightforwardly. We also examine two methods that are not perfectly captured by this taxonomy.

2. Kinematic Loop Methods

2.1. Open-Loop Calibration

The primary calibration method has been open-loop kinematic calibration, in which a manipulator is placed in a number of poses and the complete or partial end-point pose is measured (Mooring et al. 1991). The phrase *open-loop* refers to an end point that is positioned freely in space. In the following, the developments are presented for all-rotary joint manipulators but are easily recast to include prismatic joints. For a single-loop L-link manipulator, the forward kinematic equation using the Denavit-Hartenberg (1955) (DH) kinematic parameters is:

$$\mathbf{x}^i = \mathbf{g}(\boldsymbol{\theta}^i, \boldsymbol{\alpha}, \mathbf{a}, \mathbf{s}), \tag{1}$$

where $\mathbf{x}^i$ = the 6-vector for end-point position and orientation (e.g., Euler angles), i = the pose number for $1 \leq i \leq P$, P = the total number of poses, L = the number of manipulator links, $\mathbf{g}$ = the corresponding forward kinematics vector function, $\boldsymbol{\theta}^i$ = the vector of joint angles, $\boldsymbol{\alpha}$ = the vector of skew angles between neighboring joint axes, $\mathbf{a}$ = the vector of distances between joint axes along their common normals, and $\mathbf{s}$ = the vector of offsets along joint axes between neighboring common normals. To locate an arbitrary tool frame in the end point, an extra DH frame is required to yield the required six parameters; thus two parameters can be conveniently set to some simplifying constants. Moreover, a metrology system will often have an intrinsic coordinate system with respect to which measurements are made, and this coordinate system must be related to the robot's base. Thus, the dimensions of the DH parameter vectors are usually $N = L + 2$. Although a variety of kinematic parameterizations have been proposed, the use of DH parameters is quite sufficient (Hollerbach 1989). The case of nearly parallel neighboring joint axes is well handled by using the modified Hayati parameters (Hayati and Mirmirani 1985).

The DH parameters represent the geometric components of the kinematic parameters. There are additionally nongeometric components, due primarily to joint characteristics, that make the true joint angles different from the joint sensor readings. We adopt the simple example:

$$\boldsymbol{\theta}^i = \text{diag}\,(\mathbf{k})\boldsymbol{\psi}^i + \boldsymbol{\gamma}, \tag{2}$$

where $\boldsymbol{\psi}^i$ = the vector of joint angle sensor readings, $\boldsymbol{\gamma}$ = the vector of joint angle offsets, and $\mathbf{k}$ = the vector of joint angle gains. In case there are transmission elements such as gears, one may also have to account for other nongeometric factors such as gear stiffness, eccentricity, and backlash (Whitney et al. 1986).

Suppose for expository purposes that the joint model (2) is sufficient and is now substituted into (1). Also, lump all unknown kinematic parameters into a vector $\boldsymbol{\phi}$:

$$\mathbf{x}^i = \mathbf{g}^i(\boldsymbol{\psi}^i, \boldsymbol{\phi}), \tag{3}$$

where $\boldsymbol{\phi} = (\boldsymbol{\alpha}, \mathbf{a}, \mathbf{s}, \boldsymbol{\gamma}, \mathbf{k})$ and R = the dimension of $\boldsymbol{\phi}$. Next treat the joint position sensor readings $\boldsymbol{\psi}^i$ as constants that, along with constant or known kinematic parameters, are incorporated into a new forward kinematic function $\mathbf{f}^i$ derived from (3):

$$\mathbf{x}^i = \mathbf{f}^i(\boldsymbol{\phi}). \tag{4}$$

As discussed later, not all six components of pose are required for calibration, and (4) should be reduced in dimension to reflect partial pose measurement; the vector components would be

$$x^i_j = f^i_j(\boldsymbol{\phi}), \quad j = 1, \ldots, K, \tag{5}$$

where K = the number of measured pose components.

The mechanism is moved into a sufficient number P of poses to generate enough constraints to identify the parameters of interest. The equations are combined for all the poses:

$$\mathbf{x} = \mathbf{f}(\boldsymbol{\phi}), \tag{6}$$

where $\mathbf{x} = (\mathbf{x}^1, \ldots, \mathbf{x}^P)$ and $\mathbf{f} = (\mathbf{f}^1, \ldots, \mathbf{f}^P)$.

2.2. Closed-Loop Method

A disadvantage of the open-loop method is that an external metrology system is required. In recent years, an alternative *closed-loop* method has been proposed, whereby the end point is attached to the environment, and no external sensors are required (Bennett and Hollerbach 1988, 1989, 1991). A mechanism forms a single closed chain, which has to be mobile. Scenarios include a redundant manipulator with fixed end point or two nonredundant arms grasping. The only requirement is that the total number of degrees of freedom in the loop, including the ground degrees of freedom (DOFs), is at least seven to have mobility.

The forward kinematics apply as before, but now as loop closure equations. Because the origin in the loop can be placed anywhere in the chain, it can be placed at the end point. The kinematic equation (4) for a single pose i then becomes

$$\mathbf{0} = \mathbf{f}^i(\boldsymbol{\phi}), \tag{7}$$

where the "measured" end-point position and orientation $\mathbf{x}^i$ is zero by definition. Analogous to partial pose measurement, not all components of pose need be constrained; there may be passive unsensed degrees of freedom at the end point. Again, let K represent the dimension of (7), or the number of degrees of constraint. Combining all poses, one obtains the closed-loop counterpart to (6):

$$\mathbf{0} = \mathbf{f}(\phi). \tag{8}$$

There are some limitations. At least one length parameter must be known absolutely in order to scale the kinematic loop. End-point measurements or linear transducers for prismatic joints automatically provide this length reference. Because the end effector is constrained, the attainable configurations are restricted, and observability may be a problem. For the nongeometric parameters, joint gains provide particular problems: if the gains $\mathbf{k}$ in (2) are zero, then no joint readings ψ influence the loop closure equations. There is a strong attraction of the nonlinear optimization to this trivial solution. Bennett and Hollerbach (1990) proposed a solution to determine one of the gains independently. This problem does not normally arise in open-loop calibration, because the gain of the pose measurement is known independently.

2.3. *Unification of Open- and Closed-Loop Methods*

In Wampler and Arai (1992); and Wampler et al. (1995) a framework was suggested that unifies the open-loop and closed-loop calibration methods by casting the open-loop method as a closed-loop method. If the end point is unconstrained, an external sensor that completely measures the end-point pose may be considered to form a 6-DOF measured joint between end effector and ground. Hence the loop is closed through the sensor, and a new loop closure equation can be written from (6):

$$\mathbf{0} = \mathbf{f}(\phi) - \mathbf{x} = \mathbf{f}'(\phi), \tag{9}$$

where the external measurements $\mathbf{x}$ are treated as constants in $\mathbf{f}'$. This equation now has the same form as the closed-loop equation (8). The term *kinematic loop methods* is therefore coined to cover both the open- and closed-loop methods.

With this unification, a key issue is the number of unsensed joints in the kinematic loop. These unsensed joints may arise in two ways: (1) some joints in the physical linkage have no sensors, or (2) the end point is only partially constrained or measured. Any unsensed joints must be eliminated through kinematic constraints derived from the loop closure equations. Since in a single loop there are six loop closure equations, up to five unsensed joints are allowed in the kinematic loop, which are eliminated by using five of these equations to leave one equation for calibration at each pose.

2.4. *Multiple Closed Loops*

Recently, extensions of the closed-loop method to multiple closed loops have been proposed by several authors. One possibility for this extension is to write a loop closure equation (8) for each loop, then perform calibration with these combined equations (Wampler and Arai 1992; Wampler et al. 1995):

$$\mathbf{0} = \mathbf{f}_j(\phi), \tag{10}$$

for each loop j. One problem in combining the equations for multiple loops is to eliminate unsensed degrees of freedom.

2.5. *The Calibration Index*

A bewildering variety of kinematic calibration methods have been proposed that vary by the type of end-point sensing, the type of end-point constraints, and by the number of kinematic loops. We present a calibration index to classify all of these methods. Because all methods can be viewed as closed-loop methods, each closed-loop mechanism will have a certain number of degrees of freedom given by the mobility index (McCarthy 1990):

$$M = 6(L-1) - \sum_{i=1}^{J} D_i \tag{11}$$

where M = mobility index; L = number of links, including the base link and any extra links attached to the robot to constrain or measure its motion; J = number of joints, including those of any additional linkage added for calibration; and D_i = number of constraints at joint i. For a rotational or prismatic joint $D_i = 5$, while for a ball or spherical joint $D_i = 3$. For an external measurement system for a freely moving end effector $D_J = 0$, while for rigid attachment of the end point $D_J = 6$.

The total number of sensors S in the joints can be written as

$$S = \sum_{i=1}^{J} S_i, \tag{12}$$

where S_i = the number of sensed degrees in joint i. We impose the restriction $S_i \leq 6 - D_i$ (i.e., there cannot be more sensors than degrees of freedom at a joint). Usually $S_i = 1$ for the lower-order pairs typical of actuated joints, while $S_J = 6$ for full pose measurement of the end effector "joint" J. For an unsensed joint, such as in passive environment kinematics, $S_i = 0$.

Calibration can proceed if $S > M$—that is to say, there is redundant sensing with regard to positioning of the chain. The excess of sensed joints over mobility represents the number of equations per pose that can be used for calibration:

$$C = S - M, \tag{13}$$

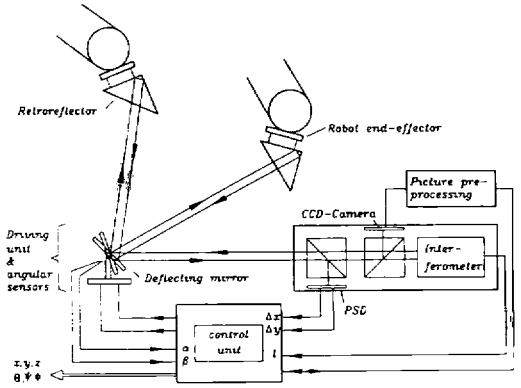

Fig. 1. Laser tracking system with orientation measurement. (From Vincze et al. [1994]).

where we term C the *calibration index*. If P is the number of poses, then CP is the total number of equations for the calibration procedure. Clearly a larger C means less poses are required, other things being equal.

For the single-loop case consisting of a series of sensed lower-order robot joints ($S_i = 1$, $D_i = 5$, $i = 1, \ldots, J-1$) with a final joint (S_J, D_J) connecting the end effector to ground, one has from eqs. (11) and (13):

$$C = S_J + D_J. \tag{14}$$

This equation shows the equivalence of end-point sensing and end-point constraints for calibration purposes.

3. Categorization by Calibration Index

We now categorize kinematic loop methods based on the calibration index C (13). For each value of C, both open and closed single-loop examples are given; in view of (14), these are discussed in terms of end-point sensing S_J and constraints D_J. When they exist, multiple closed-loop examples are discussed as well, in this case in terms of S and M. These examples are representative of recent work and are not meant to be exhaustive.

3.1. $C = 6$

For single open-loop calibration with full pose measurement, then $D_J = 0$ and $S_J = 6$. One of the most interesting recent devices for full pose measurement is the single-beam laser tracking system in Vincze et al. (1994). The robot is fitted with a retroreflector, and the laser beam is deflected by a mirror on a universal joint (Fig. 1). Position is measured using interferometry, as usual. The novel aspect is orientation measurement, by imaging of the diffraction pattern of the edges of the retroreflector. Orientation resolutions of 1 arcsec are stated, and motions can be tracked that accelerate at 100 m/s^2.

Masory et al. (1993) proposed the use of full pose measurement along with leg length measurements in the calibration of a Stewart platform ($S = 12$ and $M = 6$). The procedure is a simple extrapolation from single-loop calibration.

For single closed-loop calibration ($S_J = 0$) with rigid attachment ($D_J = 6$) of the end point to the environment, all six loop closure equations are used, and the regular open-loop calibration procedure is applied with the measured location defined to be zero in position and orientation (Bennett and Hollerbach 1988).

3.2. $C = 5$

Lau et al. (1985) presented a steerable laser interferometer with steerable reflector. With pitch and yaw measurements, the steerable interferometer yields all three components of position, while the steerable reflector yields two components of orientation ($S_J = 5$ and $D_J = 0$).

Bennett and Hollerbach (1989; 1991) considered a manipulator opening a door ($S_J = 0$ and $D_J = 5$). The door hinge angle is unsensed and must be eliminated by manipulation of the equations to leave five equations per pose. Giugovaz and Hollerbach (1994) implemented this procedure on the Sarcos Dextrous Arm; a hinge was employed to mobilize the elbow joint, which otherwise does not move during self-motions for redundant anthropomorphic manipulators with fixed end points.

Wampler et al. (1995) calibrated a Stewart platform ($M = 6$) via a closed-loop procedure. In addition to leg length measurements, all angles on one of the legs were measured ($S = 11$).

3.3. $C = 4$

We do not know of any published single-loop open or closed method for $C = 4$. Conceptually, an example in the open-loop case would be precision points involving peg-in-hole insertion, where depth and orientation are not specified. Inserting a round peg into a number of round holes in known relative locations on a table or plate would be involved.

In the closed-loop case, motion along a line with orientation constraint leaves four equations per pose. For example, the door above could also slide up and down on its hinges. Another example is a door handle turning along with the door swinging.

Bennett et al. (1990; 1991) showed that the closed loop did not need to involve physical linkages but could be formed by optical paths as virtual limbs to a stereo camera system. An uncalibrated stereo camera system could be simultaneously calibrated with an uncalibrated manipulator. Besides the two readings from its detector, each

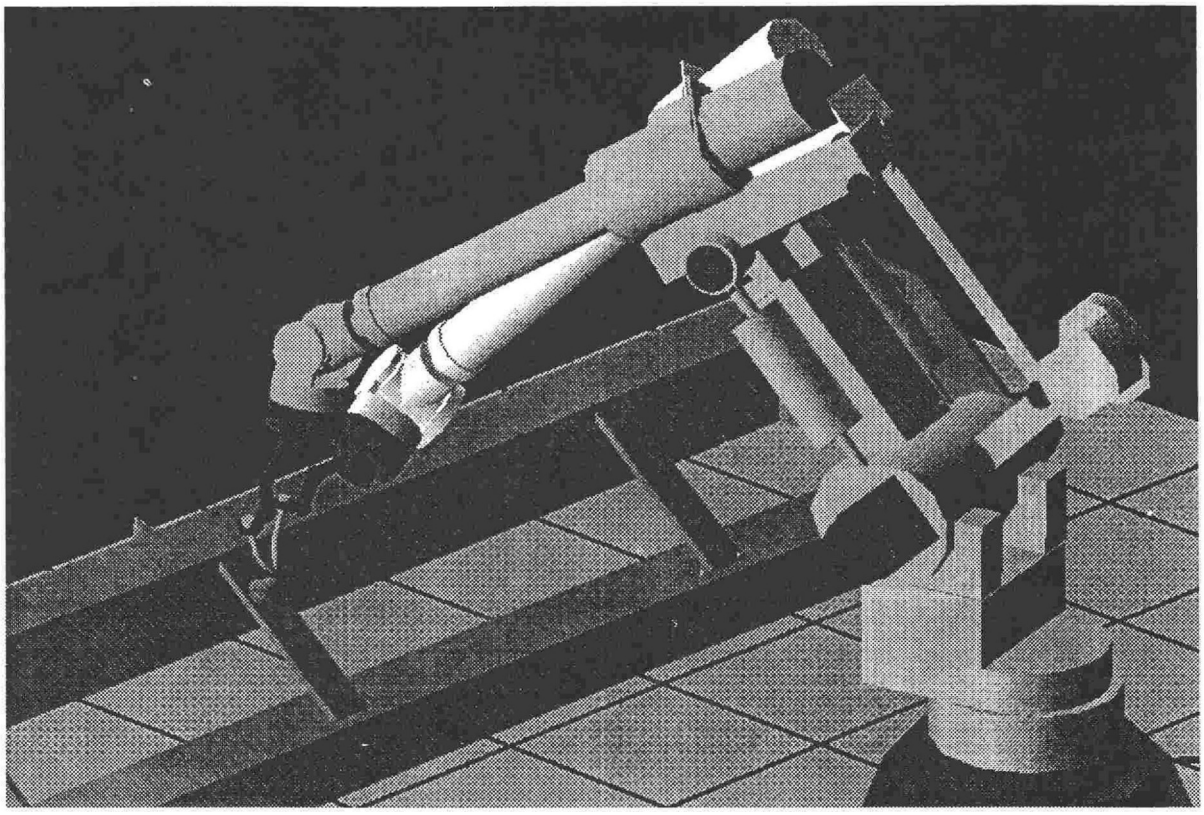

Fig. 2. A robot touching fixed fiducial points, whose relative locations are not necessarily known, in a number of orientations. (With permission from Craig [1993]).

camera was considered to have an instrumented azimuth axis ($S = 12$ for a 6-DOF arm). The ray from a tracked end point on the manipulator to the camera could be considered a link with a 3-DOF unsensed spherical joint at the end point, an unsensed sliding joint, and the 2-DOF sensed detector coordinates. Although not noted in the article, the system of manipulator with two cameras could be considered as a two-loop closed chain. Each camera, including the instrumented azimuth axis, can be considered a 7-DOF mechanism, and with the 6-DOF arm, then $M = 8$. The loop closure equation was considered as the difference between the end-point pose predicted by the manipulator versus that by the cameras, but it follows that two of the six equations used in Bennett et al. (1991) must have been redundant.

3.4. $C = 3$

Basic triangulation systems provide point measurements ($S_J = 3$ and $D_J = 0$). A recent novel device, presented by Renders et al. (1991), comprised a large-motion linear slide with small-motion orthogonal linear motions.

Bennett and Hollerbach (1989; 1991) considered point contact or manipulation of an unsensed ball joint ($S_J = 0$ and $D_J = 3$). Eliminating the unsensed DOFs is easy in this case, because the kinematic equations (8) decompose naturally into position and orientation equations. Thus, simply throw away three of the six equations in (8) having to do with orientation. Craig (1990; 1993) developed a variety of closed-loop methods, including the point contact case. A fiducial point on the end effector is touched to a fiducial point in the environment with several different orientations (Fig. 2). In an early instance of a closed-loop method, Tang (1986) proposed a two-stage method in which the angle parameters are calibrated by placing an end effector–mounted block face to face on a planar surface at several positions; this planar contact provides three constraints. Length parameters were calibrated via an open-loop approach by measuring the position of the block on the plate. If only the angle parameters are to be calibrated, then other approaches that constrain or measure orientation are conceivable—for example, using an inclinometer (or triaxial accelerometer or wrist force/torque sensor).

Hollerbach and Lokhorst (1993; 1995) autonomously calibrated a commercial hand controller with two closed loops (Fig. 3). The parameters determined were the joint angle gains and offsets as in (2) for the analog position

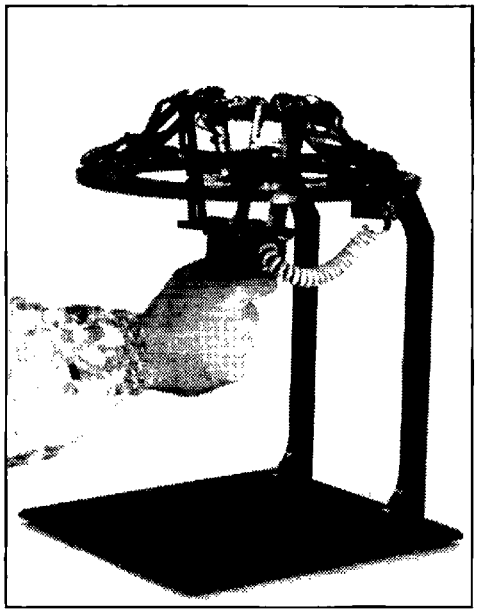

Fig. 3. RSI 6-DOF hand controller.

sensing. For this mechanism, three 6-DOF arms attach from a fixed frame to a handle ($M = 6$). In each arm, there is an unsensed spherical wrist and sensed upper arm joints ($S = 9$). The unsensed wrist joints were eliminated by formulating a fixed distance constraint between wrist points. This approach is in principle the same as using a fixed ball bar (Driels 1993), mentioned below for $C = 1$, between neighboring wrist points, where the unsensed spherical wrist joints are the kinematic equivalent of a ball joint. With regard to avoiding the trivial zero-gain solution to (2) mentioned earlier (Bennett and Hollerbach 1990), it was found that a small 10% attraction region around the correct gains exists for convergence, without assuming that one gain is known exactly. Wampler et al. (1995) reanalyzed the data using a different numerical method (see Section 4.5.2).

3.5. $C = 2$

Whitney et al. (1986) employed a single theodolite, which provides two orientation measurements: $S_J = 2$ and $D_J = 0$. A reference length had to be sighted for scaling.

Zhuang et al. (1993) developed a closed-loop procedure for calibration of a robot with a single camera mounted on the end effector. With tracking of a distinguished point in the environment, a single loop is formed, with $S_J = 2$ and $D_J = 0$. A more complicated lens model was employed than in Bennett et al. (1991), as radial distortion was parameterized through a quadratic function. Unsensed motion along a line without orientation constraints ($S_J = 0$ and $D_J = 2$) leaves two equations per pose. Newman and Osborn (1993) used a laser to define a line in space; a retroreflector mounted on the end effector reflects the laser light back to a four-quadrant detector, whose output is used to servo the manipulator to track the line.

Wampler and Arai (1992) presented simulations for a two-loop planar mechanism comprised of three prismatic legs with passive rotary joints at their ends attached to a triangular stage ($M = 3$). Leg lengths plus attachment angles for one leg were measured ($S = 5$).

3.6. $C = 1$

Several articles have recently appeared that require only one component of pose to be measured ($S_J = 1$ and $D_J = 0$). Goswami et al. (1993a,b) employed a ball bar with linear extension measured by a Linear Variable Differential Transformer (Fig. 4). Driels and Swayze (1994) used a single wire potentiometer. Tang and Liu (1993) employed a single laser displacement meter; this method requires that the laser be positioned roughly perpendicular to the flat surfaces of a stack of blocks and that the nominal parameter estimates are close to the correct estimates.

Nahvi et al. (1994) used a multiple-loop formulation to calibrate a three-loop redundantly actuated shoulder joint ($M = 3$ and $S = 4$). Boulet (1992) applied closed-loop calibration to a mechanical two-loop system formed as a single joint ($M = 1$) with two antagonistic linear actuators ($S = 2$); this device was a precursor to the shoulder joint above.

Zhuang et al. (1992) showed how a multi-beam laser tracking system, such as the Chesapeake Bay Laser System, could be calibrated by a closed loop method. This system uses triangulation to provide point measurements ($M = 3$); it has three steerable laser interferometers with retroreflector, but unlike the tracker in Lau et al. (1985), the pitch-yaw measurements are not employed. The problems with a three-beam system are (1) the relative positions of the three steerable laser interferometers must be known, and (2) interferometry provides only relative displacement, and an initial length offset must somehow be determined. Interestingly, by adding a fourth redundant tracker ($S = 4$), both the relative locations of the trackers and the initial offsets may be calibrated.

Driels (1993) employed a ball bar with known length that had unsensed spherical joints at each end. The length constraint on the ball bar yielded one calibration equation for each pose ($S_J = 0$ and $D_J = 1$). It is interesting to compare this technique to that used by Goswami et al. (1993a,b), which employs an extendable ball bar with measured radial distance. An advantage of the

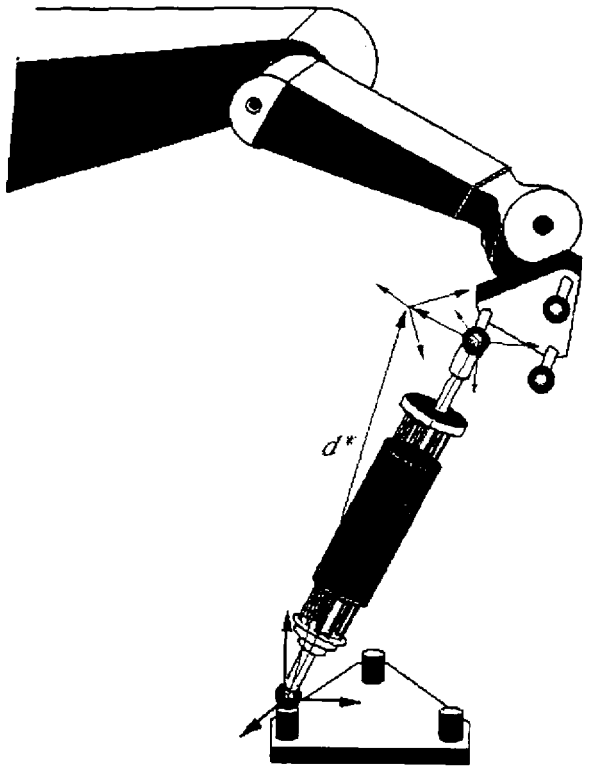

Fig. 4. Telescopic ball bar. (With permission from Goswami et al. 1993b [©*IEEE*]).

fixed-length ball bar is the lack of instrumentation; an advantage of the variable-length ball bar is the automatic adjustment to particular end-point positions and a larger set of reachable poses.

4. Numerical Methods

The final calibration accuracy will depend on the numerical methods employed. This section considers least squares methods, task variable scaling, parameter scaling, rank determination, pose selection, and handling input noise. We begin by describing the nonlinear iterative least squares method normally used to estimate the kinematic parameters.

Because robot kinematics (6) are only mildly nonlinear (Schröer 1993), linearization is an effective means for iteratively solving the nonlinear optimization and for qualitative analysis.

$$\Delta \mathbf{x} = \frac{\partial \mathbf{f}}{\partial \boldsymbol{\phi}} \Delta \boldsymbol{\phi} \equiv \mathbf{C} \Delta \boldsymbol{\phi}, \tag{15}$$

where $\Delta \mathbf{x}$ is the error between measured and computed end point position and orientation, $\mathbf{C}$ is the gradient or Jacobian, and $\Delta \boldsymbol{\phi}$ is the correction to be applied to the current parameter estimate. The ordinary least squares solution minimizes the performance index

$$J = \mathbf{e}^T \mathbf{e}, \tag{16}$$

where

$$\mathbf{e} = \mathbf{C} \Delta \boldsymbol{\phi} - \Delta \mathbf{x}. \tag{17}$$

The well-known solution is:

$$\Delta \boldsymbol{\phi} = (\mathbf{C}^T \mathbf{C})^{-1} \mathbf{C}^T \Delta \mathbf{x}. \tag{18}$$

This procedure is iterated until the corrections $\Delta \boldsymbol{\phi}$ to $\boldsymbol{\phi}$ are sufficiently small. For linearization of the closed-loop equations (8), one can use (15) exactly as before. When the manipulator is placed in different configurations with fixed end point, an incorrect kinematic model will make the end point appear to move from this fixed point. The deviation $\Delta \mathbf{x}$ from this fixed point is what is used in (15).

With the mix of DH and Hayati parameters, it is necessary to use the Levenberg-Marquardt algorithm rather than the straight Newton's method for optimization when initial parameter estimates are not accurate, because the singularity for either link labeling (parallel axes for the DH parameters, perpendicular axes for the Hayati parameters) is often encountered during the nonlinear search.

We should also briefly mention that the Jacobian $\mathbf{C}$ should not be computed directly, but for efficiency should be formed from the screw Jacobians in terms of the parameters, premultiplied by a transformation that converts from differential orthogonal rotations to differential Euler angles (Bennett and Hollerbach 1991). To avoid problems in computing Euler angles from rotation matrices and in computing the Euler angle error, it is actually best not to use differential Euler angles at all, but rather differential orthogonal rotations that directly relate to the screw Jacobian matrices. These differential orthogonal rotations can be computed directly from the difference between measured and computed rotation matrices (Hollerbach and Bennett 1988).

4.1. Task Variable Scaling

Scaling is important for good numerical performance but has not received much attention in the calibration literature. The problem of task variable scaling is well known: when performing a least squares analysis on the end-point pose error, position errors and orientation errors have to be combined. Furthermore, not all position or orientation components may be measured with equal accuracy. An ordinary least squares method (16) weighs all task variables equally. To weigh these variables differently, the general solution is left multiplication of (17) by a scaling matrix $\mathbf{G}$ (Lawson and Hanson 1974):

$$\tilde{\mathbf{e}} = \mathbf{G}\mathbf{C} \Delta \boldsymbol{\phi} - \mathbf{G} \Delta \mathbf{x} \equiv \tilde{\mathbf{C}} \Delta \boldsymbol{\phi} - \Delta \tilde{\mathbf{x}}. \tag{19}$$

Then minimize the weighted index

$$J_W = \tilde{\mathbf{e}}^T \tilde{\mathbf{e}} = \mathbf{e}^T \mathbf{G}^T \mathbf{G} \mathbf{e} \equiv \mathbf{e}^T \mathbf{W} \mathbf{e}. \quad (20)$$

The well-known weighted least squares solution is:

$$\Delta\phi = (\tilde{\mathbf{C}}^T \tilde{\mathbf{C}})^{-1} \tilde{\mathbf{C}} \Delta\tilde{\mathbf{x}} = (\mathbf{C}^T \mathbf{W} \mathbf{C})^{-1} \mathbf{C}^T \mathbf{W} \Delta\mathbf{x}, \quad (21)$$

where $\mathbf{W} = \text{diag}(\mathbf{W}_1, \ldots, \mathbf{W}_m)$. Often each $\mathbf{W}_j = \text{diag}(w_1^2, \ldots, w_k^2)$ is a diagonal weighting matrix.

4.1.1. Radians Equal Meters?

One way to choose the weighting matrix $\mathbf{W}$ is to use a priori information about acceptable relative errors. Such information might arise from specifications of the measurement apparatus. For example, Hollerbach et al. (1993) used a commercial magnetic sensor (the Bird sensor, Ascension Technology, Burlington, VT), which has a stated translational accuracy of 2.5 mm and a rotational accuracy of 10 mrad. Thus, set w_1, w_2, and w_3 to 1/2.5 mm = 400/m and w_4, w_5, and w_6 to 1/10 mrad = 100/rad.

In another approach, one should not expect to control end-point orientation better than the joint angle. If θ is the joint angle resolution, then $s = r\theta$ is the resulting end-point position resolution. For human-sized arms, $r = 1$ m and hence $s = \theta$. It seems that meters and radians are directly comparable after all! Thus, using no scaling factors for the pose parameters makes some sense and may explain why the general disregard for scaling in the robotics community has not resulted in disaster. Of course, if linkages are much smaller (like fingers) or much larger (like excavators), then the situation is different.

4.1.2. Gauss-Markov Estimate

A principled way of task variable scaling is to use the uncertainty σ_i^x in each task variable measurement x_i, should this be known: each $w_i = 1/\sigma_i^x$ for $1 \leq i \leq k$ measured pose components. The standard deviations σ_i^x are not necessarily the same as end-point measurement accuracy, because model errors and input noise also contribute to the error equation (17). The remainder of the article assumes that a Gaussian distribution is a reasonable model for measurement error and parameter variation.

In general, the measurement errors are not independent, and one must use the covariance matrix $\mathbf{R} = \boldsymbol{cov}(\mathbf{x})$. If $\mathbf{R} = \mathbf{F}\mathbf{F}^T$ is its Cholesky factorization, then define the weighting matrix $\mathbf{W} = \mathbf{F}^{-T}\mathbf{F}^{-1}$. The weighted sum of squared errors then becomes (Lawson and Hanson 1974):

$$\chi^2 = (\mathbf{F}^{-1}\mathbf{e})^T(\mathbf{F}^{-1}\mathbf{e}) = \mathbf{e}^T\mathbf{R}^{-1}\mathbf{e}. \quad (22)$$

This corresponds to left multiplication of (17) by the matrix $\mathbf{F}^{-1}$ to yield:

$$\tilde{\mathbf{e}} = \mathbf{F}^{-1}\mathbf{e} = \mathbf{F}^{-1}\mathbf{C}\Delta\phi - \mathbf{F}^{-1}\Delta\mathbf{x} \equiv \tilde{\mathbf{C}}\Delta\phi - \Delta\tilde{\mathbf{x}}. \quad (23)$$

The performance index (22) is a χ^2 statistic, whose minimization for Gaussian distributions leads to the maximum likelihood estimate (Bevington and Robinson 1992; Press et al. 1992):

$$\Delta\phi = (\mathbf{C}^T\mathbf{R}^{-1}\mathbf{C})^{-1}\mathbf{C}^T\mathbf{R}^{-1}\Delta\mathbf{x}. \quad (24)$$

This solution is variously called the *Gauss-Markov estimate*, the *generalized least squares estimate*, or the *best linear unbiased estimator* (BLUE) (Norton 1986). It is the minimum covariance estimate (on the parameter error) of all unbiased estimators. A significant point is that $\boldsymbol{cov}(\Delta\tilde{\mathbf{x}}) = \mathbf{I}$ (i.e., the uncertainty in components of $\Delta\tilde{\mathbf{x}}$ are about the same size). Hence, the Euclidean norm of the error vector $\Delta\tilde{\mathbf{x}}$ is a reasonable measure of its size.

Often we do not know the covariance matrix $\mathbf{R}$ that well. One approach is to uniformly scale an initial estimate of $\mathbf{R}$ after a preliminary calibration, based on the value of χ^2 (Bevington and Robinson 1992; Press et al. 1992). The expected value of χ^2 is $\nu = mk - r$, where m is the number of poses, k is the number of pose components, r is the number of estimated parameters, and ν is called the *degrees of freedom*. Thus, scale $\mathbf{R}$ by ν/χ^2. Another approach is to treat the elements of $\mathbf{R}$ as additional variables to be estimated when (22) is minimized. The solution is then a pair of coupled nonlinear equations (Norton 1986) that yields both $\Delta\phi$ and $\mathbf{R}$.

4.2. Parameter Scaling

With regard to parameter scaling, in related applications such as redundancy resolution, problems created by improper scaling of joint variables have been identified (Doty et al. 1993). For example, sliding joint and rotary joint variables cannot be directly combined when finding the minimum-norm least squares solution to the joint rates. In kinematic calibration the least squares problem is overconstrained, and hence there is no parameter null space that can be added to a nominal parameter solution to adjust some norm. Nevertheless, scaling is important for proper convergence in nonlinear optimization and for singular value decomposition. One wishes to examine the singular values for such reasons as optimum poses selection (Borm and Menq 1991) and elimination of redundant or unidentifiable parameters (Schröer 1993). Yet, if parameters have vastly different magnitudes, then the singular values are not directly comparable. Another use of parameter scaling is incorporation of a priori information about likely parameter values into the performance index.

Whereas left multiplication of the Jacobian $\mathbf{C}$ in (23) results in task variable scaling, right multiplication of $\mathbf{C}$ by a weighting matrix $\mathbf{H}$ results in parameter scaling (Lawson and Hanson 1974):

$$\Delta\mathbf{x} = (\mathbf{CH})(\mathbf{H}^{-1}\Delta\boldsymbol{\phi}) \equiv \bar{\mathbf{C}}\Delta\tilde{\boldsymbol{\phi}}. \tag{25}$$

4.2.1. Column Scaling

The most common approach toward parameter weighting is column scaling, which does not require a priori statistical information. Define a diagonal matrix $\mathbf{H} = \text{diag}(h_1, \ldots, h_r)$ with elements

$$h_j = \begin{cases} \|\mathbf{c}_j\|^{-1} & \text{if} \|\mathbf{c}_j\| \neq 0 \\ 1 & \text{if} \|\mathbf{c}_j\| = 0 \end{cases} \tag{26}$$

where $\mathbf{c}_j$ is the jth column of $\mathbf{C}$. Then (25) becomes:

$$\Delta\mathbf{x} = \sum_{j=1}^{r} \frac{\mathbf{c}_j}{\|\mathbf{c}_j\|}\Delta\phi_j\|\mathbf{c}_j\|. \tag{27}$$

Suppose $\Delta\mathbf{x}$ has been previously normalized; then its length is meaningful. Each $\mathbf{c}_j/\|\mathbf{c}_j\|$ is a unit vector, and hence each $\Delta\phi_j\|\mathbf{c}_j\|$ is about the same size and has the same effect on $\Delta\mathbf{x}$.

Schröer (1993) identified a problem with column scaling—namely, that bad identifiability of parameters can result in very small Euclidean norms, which result in very large scaling factors. This results in strong amplification of uncertainties of $\mathbf{C}$. Instead, Schröer proposes scaling based on the effect on the anticipated error of the robot (say, 1 mm). From (17), for each pose i the end-point error due to the parameter component change $\Delta\phi_j$ is:

$$\|\Delta\mathbf{x}^i\|^2 = (\Delta\phi_j)^2\|\mathbf{c}_j^i\|^2, \tag{28}$$

where $\mathbf{c}_j^i$ is extracted from $\mathbf{c}^i$. The scaling factor $\sigma\phi_j^i$ is defined as that parameter deviation that causes a 1-mm end-point displacement; i.e.,

$$\sigma\phi_j^i = \frac{10^{-3}m}{\|\mathbf{c}_j^i\|}. \tag{29}$$

The pose displacement $\Delta\mathbf{x}^i$ must have been previously normalized; alternatively, just use its first three position components. The scale factor $\sigma\phi_j^i$ is clearly pose dependent. The most conservative estimate $\sigma\phi_j$ over all poses is called the *extremal scaling value* (Schröer et al. 1992; Schröer 1993):

$$\sigma\phi_j = \min_i \left\{\sigma\phi_j^i\right\}. \tag{30}$$

Then define the scaling matrix $\mathbf{H} = \text{diag}(\sigma\phi_1, \ldots, \sigma\phi_r)$.

4.2.2. Scaling by Parameter Covariance

In an ideal case, one would have a priori knowledge of the expected value $\boldsymbol{\phi}_0$ of the parameter vector and the standard deviation σ_j^{ϕ} of each of the parameter vector components. Define $\boldsymbol{\phi} = \boldsymbol{\phi}_0 + \boldsymbol{\phi}_e$, where $\boldsymbol{\phi}$ is the true parameter value vector and $\boldsymbol{\phi}_e$ is the error (Wampler et al. 1995). Incorporate $\boldsymbol{\phi}_0$ as constants into (6), which then becomes $\mathbf{x} = \mathbf{f}(\boldsymbol{\phi}_e)$. The problem now is to estimate the error $\boldsymbol{\phi}_e$ by iterative least squares, adding corrections $\Delta\boldsymbol{\phi}_e$ as in (18). Define a weighting matrix $\mathbf{H} = \text{diag}(\sigma_1^{\phi}, \ldots, \sigma_r^{\phi})$ in (25).

More generally, the parameter distribution would be described by a covariance matrix $\mathbf{M} = cov(\boldsymbol{\phi}_e)$. As before, one can find a Cholesky factorization $\mathbf{M} = \mathbf{HH}^T$, and this $\mathbf{H}$ can now be applied in (25) to yield a scaled $\tilde{\boldsymbol{\phi}}_e = \mathbf{H}^{-1}\boldsymbol{\phi}_e$. Then $cov(\tilde{\boldsymbol{\phi}}_e) = \mathbf{I}$, and hence the parameters are scaled evenly and are now comparable.

After calibration, a revised estimate $\hat{\mathbf{M}}$ of the covariance can be derived from the data (Norton 1986). This estimate can be used for subsequent singular value decomposition analysis for rank reduction. Assume that the task variables $\Delta\mathbf{x}$ have been previously scaled for equal uncertainty σ, that there is no bias ($E\mathbf{e} = 0$), and that the errors are uncorrelated ($cov(\mathbf{e}) = \sigma^2\mathbf{I}$). Then

$$\hat{\mathbf{M}} = \sigma^2(\mathbf{C}^T\mathbf{C})^{-1}, \tag{31}$$

where again an unbiased estimator for σ^2 from (22) and (24) is $\hat{\sigma}^2 = \chi^2/\nu$. This equation is also valid if $\mathbf{C}$ is replaced by $\tilde{\mathbf{C}}$ from (23).

4.2.3. Damped Least Squares

Ordinary or weighted least squares treat parameter values as completely unknown (i.e., they could be anywhere in the range from $-\infty$ to $+\infty$). Yet often a fairly good initial estimate of the parameters is available—for example, from a manufacturer's specifications or in case of a recalibration. It makes sense to incorporate such an a priori preference $\boldsymbol{\phi}_0$ into the least squares optimization (Lawson and Hanson 1974). To capture the notion of nearness, scale the squared parameter residual by a matrix $\mathbf{K}$. Then augment the weighted least squares criterion:

$$J_{WK} = \mathbf{e}^T\mathbf{We} + \lambda^2\Delta\boldsymbol{\phi}_e^T\mathbf{K}\Delta\boldsymbol{\phi}_e. \tag{32}$$

The constant λ is a relative weighting factor that one may choose based on confidence in the nominal solution. This formulation has the form of damped least squares, with solution

$$\Delta\boldsymbol{\phi}_e = (\mathbf{C}^T\mathbf{WC} + \lambda^2\mathbf{K})^{-1}\mathbf{C}^T\mathbf{W}\Delta\mathbf{x}. \tag{33}$$

Another use of damped least squares, when $\mathbf{K} = \mathbf{I}$, the identity matrix, is to circumvent singularities in the DH

parameterization during iterative search (Bennett and Hollerbach 1991).

When $\lambda = 1$ and the end-point errors and parameter deviations are both weighted by their uncertainties, the performance index (32) is again a χ^2 statistic:

$$\chi^2 = \mathbf{e}^T\mathbf{R}^{-1}\mathbf{e} + \Delta\boldsymbol{\phi}_e^T\mathbf{M}^{-1}\Delta\boldsymbol{\phi}_e. \tag{34}$$

Its solution is the minimum variance estimate, which, unlike (24), is biased:

$$\Delta\boldsymbol{\phi} = (\mathbf{C}^T\mathbf{R}^{-1}\mathbf{C} + \mathbf{M}^{-1})^{-1}\mathbf{C}^T\mathbf{R}^{-1}\Delta\mathbf{x}. \tag{35}$$

The Kalman filter recursively solves the same problem (Luenberger 1969; Sorenson 1970): when the state is nonvarying, there is a constant process, and there is no process noise (Mooring et al. 1991; Roth et al. 1987). The Gauss-Markov estimate is the limiting case when $\mathbf{M}^{-1}$ is zero (i.e., there is no a priori information about the parameters). Again, there is an issue of determining the covariances. As for the Gauss-Markov estimate, the expected value of χ^2 can be used to uniformly scale $\mathbf{R}$ and $\mathbf{M}$ post facto (Bryson and Ho 1975).

4.3. *Rank Determination*

Once all parameters have been scaled, singular value decomposition can be properly used to determine identifiability of the kinematic parameters because the singular values are now comparable.

$$\mathbf{C} = \mathbf{U}\boldsymbol{\Sigma}\mathbf{V}^T, \tag{36}$$

where $\mathbf{C}$ has dimensions $p \times q$, $\mathbf{U}$ is a $p \times q$ column-orthogonal matrix, $\mathbf{V}$ is a $q \times q$ orthogonal matrix, and $\boldsymbol{\Sigma} = \text{diag}(\mu_1, \ldots, \mu_r, 0, \ldots, 0)$ is the $q \times q$ matrix of ordered singular values, with μ_1 the largest and μ_r the smallest nonzero singular value.

Especially when complex joint models are assumed that include flexibility, backlash, and gear eccentricity, it is not clear that all parameters can be identified. Retaining poorly identifiable parameters will degrade the robustness of the calibration; such parameters are indicated by zero or very small singular values. The expansion of (15) in terms of (36) is

$$\Delta\mathbf{x} = \sum_{j=1}^{r} \mu_j(\mathbf{v}_j^T\Delta\boldsymbol{\phi})\mathbf{u}_j, \tag{37}$$

where $\mathbf{u}_j$ and $\mathbf{v}_j$ are the jth columns of $\mathbf{U}$ and $\mathbf{V}$. For zero or small singular values μ_j, the projection $\mathbf{v}_j^T\Delta\boldsymbol{\phi}$ of the parameters onto the column vector $\mathbf{v}_j$ represents a linear combination of parameters that cannot be identified independently. Three methods to proceed are as follows:

1. Explicitly removing poorly identifiable parameters by analyzing these linear combinations. With the parameters properly scaled using extremal scaling values, Schröer (1993) suggests the heuristic that the resulting condition number should be less than 100:

$$\kappa(\mathbf{C}) = \frac{\mu_1}{\mu_r} < 100. \tag{38}$$

This heuristic derives from their experience and from that of their statistical community. To proceed by eliminating parameters, examine the linear sums (37) corresponding to the smallest singular value μ_r. Sometimes it is obvious which parameter in the projection should be eliminated, but often it is not, because the parameters may not differ that much in magnitude. Schröer (1993) suggests the use of sensitivity values ${}^x\sigma_j^\phi$ for each parameter, defined as follows. In (31), for the purposes of relative comparison between parameters, assume $\sigma = 1$. Then σ_j^ϕ is the root of the jth diagonal element of $cov(\Delta\hat{\boldsymbol{\phi}})$. These standard deviations are made dimensionless by using the mean scaling values $\bar{\sigma}\phi_j$, the mean of all values (29) over all the poses:

$$\bar{\sigma}\phi_j = \frac{1}{m}\sum_{i=1}^{m}\sigma\phi_j^i. \tag{39}$$

The sensitivity value ${}^x\sigma_j^\phi$ normalizes the parameter standard deviations σ_j^ϕ by their mean scaling values $\bar{\sigma}\phi_j$:

$${}^x\sigma_j^\phi = \frac{\sigma_j^\phi}{\bar{\sigma}\phi_j}. \tag{40}$$

Parameters with the largest sensitivities are candidates for elimination. In this procedure, the unscaled singular values are employed.

2. Zeroing small singular values. One may proceed without first removing parameters. For weighted least squares the solution to (21) is (Press et al. 1992):

$$\Delta\boldsymbol{\phi} = \sum_{j=1}^{n}\frac{\mathbf{u}_j^T\tilde{\mathbf{x}}}{\mu_j}\mathbf{v}_j \tag{41}$$

If μ_j is zero or very small, then set $1/\mu_j = 0$.

3. Incorporating a priori parameter estimates. For damped least squares, no explicit action on the singular values is required, because the damping factor modifies the singular values; for example, for $\mathbf{K} = \mathbf{I}$ in (33), then

$$\Delta\boldsymbol{\phi} = \sum_{j=1}^{n}(\mathbf{u}_j^T\tilde{\mathbf{x}})\frac{\mu_j}{\mu_j^2 + \lambda^2}\mathbf{v}_j. \tag{42}$$

Hence, a very small μ_j is counteracted by the larger λ value; then the a priori information about parameter values dominates the information from the data (i.e., the data are ignored).

4.4. Pose Selection

Good pose sets should lead to the best observability of the parameters (i.e., the most accurate estimates). Major approaches toward quantifying observability involve an analysis of the singular values (36): the observability index (Borm and Menq 1991), the condition number (Driels and Pathre 1990), and the minimum singular value (Nahvi et al. 1994).

Assume that the rank has been determined and is r. Borm and Menq (1991) have proposed the observability index O_{BM}, which maximizes the product of all of the singular values:

$$O_{BM} = \frac{\sqrt[r]{\mu_1 \cdots \mu_r}}{\sqrt{m}}. \tag{43}$$

The rationale is that O_{BM} represents the volume of a hyperellipsoid in $\Delta\mathbf{x}$, defined by (15) when $\Delta\phi$ defines a hypersphere, and the singular values from (36) represent the lengths of axes. Therefore, maximimizing O_{BM} gives the largest hyperellipsoid volume and, hence, a good aggregate increase of the singular values. One can also derive O_{BM} from the well-known relation $\sqrt{det(\mathbf{C}^T\mathbf{C})} = \mu_1 \cdots \mu_r$.

Driels and Pathre (1990) have proposed minimizing the condition number of $\mathbf{C}$ as a measure of observability:

$$O_\kappa = \mu_1/\mu_r. \tag{44}$$

This measure addresses the eccentricity of the hyperellipsoid rather than its size. The intermediate singular values are not considered to be that pertinent, because minimizing the condition number automatically makes all singular values become more similar in magnitude and makes the hyperellipsoid closer to a hypersphere.

Nahvi et al. (1994) argue for maximizing the minimum singular value μ_r as an observability measure:

$$O_{msv} = \mu_r. \tag{45}$$

The rationale is to make the shortest axis as long as possible, regardless of the other axes—that is to say, to improve the worst case. Consider the following standard result:

$$\mu_r \leq \frac{\|\Delta\mathbf{x}\|}{\|\Delta\phi\|} \leq \mu_1, \tag{46}$$

or more particularly,

$$\mu_r\|\Delta\phi\| \leq \|\Delta\mathbf{x}\|. \tag{47}$$

Then maximizing μ_r ensures that a given size of parameter errors $\|\Delta\phi\|$ has the largest possible influence on the pose errors $\|\Delta\mathbf{x}\|$. Hollerbach and Lokhorst (1995) applied these three observability measures and found that the condition number and the minimum singular value gave about the same good result: their relative magnitudes were almost proportional to the rms errors of the final parameter errors. The observability index O_{BM} was not as sensitive and not directly related to rms parameter errors.

These observability measures have direct parallels in the literature on dexterity measures for redundancy resolution of manipulators (Table 1). The manipulability index $\sqrt{det(\mathbf{J}\mathbf{J}^T)} = \mu_1 \cdots \mu_l$ has been proposed (Yoshikawa 1985) to quantify configurations, where $\mathbf{J}$ is the rank l Jacobian and the μ_js are its singular values. The manipulability index is directly analogous to the observability index O_{BM}, as they both involve the product of the singular values. When the manipulability index is zero, the manipulator is at a singular configuration, but it has been argued that the actual value of the determinant cannot be used as a practical measure of ill conditioning (Klein and Blaho 1987). Alternatively, the condition number $\kappa(J) = \mu_1/\mu_l$ was proposed in Salisbury and Craig (1982), and the minimum singular value in Klein and Blaho (1987). A comparative analysis by Klein and Blaho (1987) of all three dexterity measures concluded that the manipulability index had some disadvantages, while the condition number and minimum singular value gave good quantitative results and were complementary. This seems to accord with the results of Nahvi et al. (1994).

4.5. Handling Input Noise

As mentioned earlier, in the least squares formulation (17) only output noise (in the measured pose components) is considered. If input noise (in the joint angles) is significant, then bias errors may result; the Appendix provides a synopsis from Norton (1986) that demonstrates this important fact. With few exceptions, this potential problem does not yet appear to have been generally addressed in the calibration literature.

As a simple example, consider the linear equation $y = ax$, where only the slope a is to be determined. If the uncertainties in the input/output variables are σ_x and σ_y, then the weighted normal distances from points (x_i, y_i) to the line are minimized:

$$\chi^2 = \sum_{i=1}^{P} \frac{(y_i - ax_i)^2}{\sigma_y^2 + a^2\sigma_x^2}, \tag{48}$$

which is a χ^2 statistic (Bevington and Robinson 1992; Press et al. 1992). To solve this equation, Press et al.

Table 1. Analogies between Dexterity Measures for Redundancy Resolution and Observability Measures for Pose Selection.

Dexterity Measure	Observability Measure
Manipulability index (Yoshikawa 1989) $\mu_1 \cdots \mu_l$	Observability index (Borm and Menq 1991) $\sqrt[r]{\mu_1 \cdots \mu_r}/\sqrt{m}$
Condition number (Salisbury and Craig 1982) μ_1/μ_l	Condition number (Driels and Pathre 1990) μ_1/μ_r
Minimum singular value (Klein and Blaho 1987) μ_l	Minimum singular value (Nahvi et al. 1994) μ_r

(1992) proposed an iterative nonlinear optimization procedure.

The formulation and solution of equations such as (48) have appeared under various names and guises over the years, including total least squares (Van Huffel and Vandewalle 1991), orthogonal distance regression (Boggs et al. 1987), or errors-in-variables regression (Fuller 1987). One common application is to fit a plane to a set of measured 3D points; all three components of measured position have noise. For example, this problem arises when measuring multiple points on an end effector and establishing a coordinate system (e.g., An et al. 1988). Another example is circle point analysis, where a plane is to be fitted to the circle of points generated by moving a single joint (Mooring et al. 1991). Total least squares solves such equations analytically using singular value decomposition, making unnecessary the iterative solution proposed in Press et al. (1992).

4.5.1. *Nonlinear Total Least Squares*

Even more pertinent to kinematic calibration, nonlinear versions of the total least squares problem have been developed. As another simple example, suppose we are now trying to fit a scalar function $y = f(x, a)$ by adjusting some parameters a (Boggs et al. 1987). Assuming again equivalent error in x and y measurements, we should minimize the Euclidean distances from the measurements to the fitted curve f (Fig. 5).

Particularized to calibration, the underlying forward kinematics function derived for all poses from (3) is written to reflect both the input $\Delta\psi$ and output $\Delta\mathbf{x}$ measurement errors:

$$\mathbf{x} - \Delta\mathbf{x} = \mathbf{g}(\psi - \Delta\psi, \phi), \tag{49}$$

where again $\mathbf{g} = (\mathbf{g}_1, \ldots, \mathbf{g}_M)$ is the stacked vector for all poses. Let the covariances of the input and output variables be $\mathbf{R} = \mathbf{E}(\Delta\mathbf{x}\Delta\mathbf{x}^T)$ and $\mathbf{P} = \mathbf{E}(\Delta\psi\Delta\psi^T)$. Then

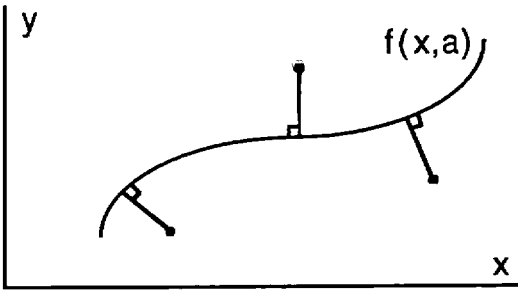

Fig. 5. Fitting a curve $y = f(x, a)$ with both input and output errors.

we minimize the weighted orthogonal squared distances from the measurements $(\mathbf{x}, \psi)$ to the multidimensional surface represented by $\mathbf{x} = \mathbf{g}(\psi, \phi)$:

$$\min_{\phi, \Delta\mathbf{x}, \Delta\psi} \chi^2 = \Delta\mathbf{x}^T\mathbf{R}^{-1}\Delta\mathbf{x} + \Delta\psi^T\mathbf{P}^{-1}\Delta\psi \tag{50}$$

subject to (49). The solution proceeds by substituting (49) into (50) to eliminate $\Delta\mathbf{x}$:

$$\min_{\phi, \Delta\psi} \chi^2 = (\mathbf{x} - \mathbf{g}(\psi - \Delta\psi, \phi))^T\mathbf{R}^{-1} \times(\mathbf{x} - \mathbf{g}(\psi - \Delta\psi, \phi)) + \Delta\psi^T\mathbf{P}^{-1}\Delta\psi, \tag{51}$$

which is an unconstrained optimization problem, solved as usual by linearization and iteration (Schwetlick and Tiller 1985).

Such an approach for robot calibration was taken by Zak et al. (1994), who augmented the output variance in the linearized equations (23) with the transformed input variance as follows:

$$\tilde{\mathbf{R}} = \mathbf{R} + \mathbf{J}\mathbf{P}\mathbf{J}^T, \tag{52}$$

where $\mathbf{J} = \text{diag}(\mathbf{J}^1_\psi, \ldots, \mathbf{J}^P_\psi)$ is a block-diagonal matrix whose elements $\mathbf{J}^i_\psi$ are the Jacobians of $\mathbf{g}^i$ with regard to the joint angle sensors ψ at pose i. This weighting equation is the generalization of the weighting in (48).

Zak et al. (1994) then apply the Gauss-Markov estimate (24) iteratively, at each step treating $\mathbf{J}$ (which contains the unknown parameters) as a constant matrix based on the current estimates, and obtaining the Gauss-Markov estimate (24) with the modified $\tilde{\mathbf{R}}$.

4.5.2. *Implicit Loop Method*

Renders et al. (1991) and Wampler et al. (1995) proposed methods for kinematic calibration equivalent to nonlinear total least squares, with the addition of a priori parameter estimates as in damped least squares. Following the development in Wampler et al. (1995), an implicit equation results from the unifying view of open-loop kinematic calibration methods as closed-loop methods. Because end-point measurements are considered as a joint, all measurements, whether from joint angle sensors or end-point sensors, are grouped together into a vector $\mathbf{x} = \mathbf{x}_0 + \mathbf{x}_e$, where $\mathbf{x}_0$ is the measurement and $\mathbf{x}_e$ is the measurement error. Also, set $\phi = \phi_0 + \phi_e$. Incorporate $\mathbf{x}_0$ and ϕ_0 as constants into the loop closure equation (9), which is then a function $\mathbf{f}'(\mathbf{x}_e, \phi_e) = \mathbf{0}$. The maximum likelihood estimate minimizes

$$\chi^2 = \mathbf{x}_e^T \mathbf{R}^{-1} \mathbf{x}_e + \phi_e^T \mathbf{M}^{-1} \phi_e \tag{53}$$

subject to $\mathbf{f}'(\mathbf{x}_e, \phi_e) = \mathbf{0}$, where $E(\mathbf{x}_e \mathbf{x}_e^T) = \mathbf{R}$.

This minimization problem is solved by linearization of the constraints and iteration. Let the scaled variables $\mathbf{y}$ and $\mathbf{q}$ be defined via $\mathbf{x}_e = \mathbf{R}^{1/2}\mathbf{y}$ and $\phi_e = \mathbf{M}^{1/2}\mathbf{q}$, where the superscript $^1/_2$ means the symmetric square root. Iterate from an initial guess $\mathbf{y} = \mathbf{0}$ and $\mathbf{q} = \mathbf{0}$ to find corrections $\Delta\mathbf{y}$ and $\Delta\mathbf{q}$ to minimize

$$\chi^2 = (\mathbf{y} + \Delta\mathbf{y})^T (\mathbf{y} + \Delta\mathbf{y}) + (\mathbf{q} + \Delta\mathbf{q})^T (\mathbf{q} + \Delta\mathbf{q}) \tag{54}$$

subject to the linearized constraints

$$-\mathbf{f}'(\mathbf{y}, \mathbf{q}) = \frac{\partial \mathbf{f}'}{\partial \mathbf{y}}(\mathbf{y}, \mathbf{q})\Delta\mathbf{y} + \frac{\partial \mathbf{f}'}{\partial \mathbf{q}}(\mathbf{y}, \mathbf{q})\Delta\mathbf{q} \equiv \mathbf{J}_y \Delta\mathbf{y} + \mathbf{J}_q \Delta\mathbf{q}. \tag{55}$$

Compute the QR-decomposition $\mathbf{Q}\tilde{\mathbf{R}} = \mathbf{J}_y^T$ (this is actually done individually for each pose) and define

$$\mathbf{D} = \tilde{\mathbf{R}}^{-T} \mathbf{J}_y, \quad \mathbf{E} = \mathbf{Q}^T \mathbf{y} - \tilde{\mathbf{R}}^{-T} \mathbf{f}'(\mathbf{y}, \mathbf{q}). \tag{56}$$

The variables $\Delta\mathbf{y}$ are eliminated and the step in $\mathbf{q}$ found from:

$$\begin{bmatrix} \mathbf{D} \\ \mathbf{I} \end{bmatrix} \Delta\mathbf{q} = \begin{bmatrix} \mathbf{E} \\ -\mathbf{q} \end{bmatrix} \tag{57}$$

and the updated error estimates are

$$\mathbf{y} + \Delta\mathbf{y} = \mathbf{Q}(\mathbf{E} - \mathbf{D}\mathbf{q}). \tag{58}$$

Covariance matrices are again scaled post facto based on the value of χ^2.

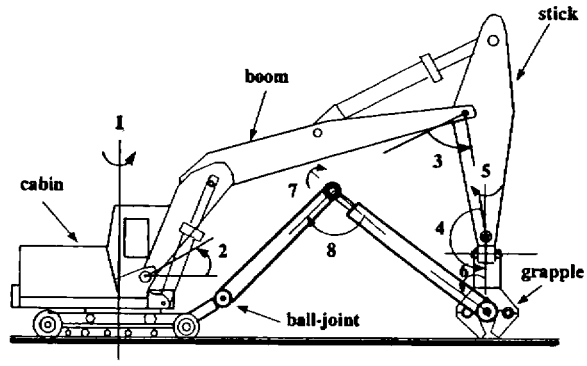

Fig. 6. Excavator with calibrator.

Because the loop closure equation (9) is an implicit function of all measurements, Wampler et al. (1995) coined the term *implicit loop method.* Whereas in nonlinear total least squares (50) the output errors could be directly eliminated by using the explicit constraint equation, for the implicit loop method the linearization of the implicit constraint equation was required for this elimination. The earlier approach of Renders et al. (1991) deals only with open-loop calibration of serial arms; the resulting explicit constraint equation is incorporated using Lagrange multipliers rather than using variable elimination as in (50). As in Zak et al. (1992), linearization is at nominal values, whereas in the implicit loop method the unknown parameters from the linearization also come into play.

5. Screw Axis Measurement

Screw axis measurement methods proceed quite differently from the kinematic loop methods. Each joint axis is identified as a screw (i.e., as a line in space). From a knowledge of all of the joint screws, the kinematic parameters can be quite straightforwardly extracted.

5.1. *Circle Point Analysis*

The main screw axis measurement method has been *circle point analysis* (CPA), where each joint is moved individually in a circle (Mooring et al. 1991). The normal of the plane in which the circle lies and the center of the circle define the joint screw. In the past, position measurements of a point on the end effector have been used to define each circle (Stone 1987). In biomechanics, CPA is often performed to find the instantaneous center of rotation of a joint (Woltring et al. 1985).

In Khoshzaban et al. (1992), a teleoperated log-loader with four unsensed joints (joints 1–4 in Figure 6) was

calibrated using an additional 7-DOF linkage termed a *calibrator*. Joints 5–8 of the calibrator are sensed, where joint 5 is attached to the grapple; the ball-joint attachment to the base is a 3-DOF unsensed joint. The log-loader arm joints are moved one at a time for calibration. The authors were successful in formulating a recursive closed-loop procedure to effect the calibration, working from distal to proximal log-loader joints. Using the same data, it would also have been possible to formulate a CPA approach. The fixed base could be considered to be at the grapple, and the ball-joint could be considered as moving in a circle with individual log-loader joint movement. The 3D position coordinates of the ball joint would be provided by the measured calibrator joints.

Instead of direct position measurement, another approach to CPA is the use of a triaxial accelerometer at the end point (Canepa et al. 1994), whose output is integrated. With the highly accurate accelerometers currently on the market, precise calibration appears possible. Their advantage is portability and lack of viewing constraints.

One complication in CPA is that there has to be a guarantee that the nonmoving joints are indeed stationary. If the joint has gears, a brake on the output shaft would be necessary. If the brake is on the input shaft, gear deflection during motion would change the joint angle. If there is no brake, a very stiff servo with integral control would be necessary, and sufficient settling time must be allowed. If measurements are to be taken during a trajectory, then some form of iterative learning scheme is probably necessary (An et al. 1988). Perhaps as a result, to date CPA has been applied only to the geometric factors.

Another limitation is that the base parameters s_1 and θ_1 cannot be determined, because in the first joint screw the axis $\mathbf{x}_0$ does not play a role. The problem is not serious, because the base coordinate location is arbitrary, and so are these parameters.

Different procedures have been proposed to extract the kinematic parameters from a knowledge of the joint axes (Mooring et al. 1991; Stone 1987). An elegant method has been put forth by Sklar (1989), not well publicized except in Mooring et al. (1991). Let each joint screw S_j be represented as

$$S_j = \begin{bmatrix} \mathbf{z}_{j-1} \\ \mathbf{z}_{j-1} \times \mathbf{b}_j \end{bmatrix}, \tag{59}$$

where $\mathbf{z}_{j-1}$ is the joint j axis vector and $\mathbf{b}_j$ is a vector from this axis to a fixed reference frame, such as the end point or an external measurement system. Then the reciprocal product of adjacent screws (Roth 1984), called the *mutual moment* by Sklar (1989), when evaluated in terms of Denavit-Hartenberg (DH) parameters is

$$S_j \circ S_{j+1} = -a_j \sin \alpha_j, \tag{60}$$

where α_j is the skew angle and a_j is the distance along $\mathbf{x}_j$ between $\mathbf{z}_{j-1}$ and $\mathbf{z}_j$. By definition, $\mathbf{x}_j$ points in the direction of $\mathbf{z}_j$ from $\mathbf{z}_{j-1}$; hence a_j by construction is never negative. Yet we cannot determine from $\mathbf{z}_{j-1} \times \mathbf{z}_j = \mathbf{x}_j \sin \alpha_j$ which way $\mathbf{x}_j$ should point. The mutual moment (60) yields this information: if negative, then the direction is $\mathbf{z}_{i-1} \times \mathbf{z}_i$; if positive, $\mathbf{z}_j \times \mathbf{z}_{j-1}$. If $S_j \circ S_{j+1} = 0$, then one can determine from $|\mathbf{z}_{j-1} \times \mathbf{z}_j| = \cos \alpha_j$ whether $a_j = 0$ or $\sin \alpha_j = 0$. Thus, we can tell the quadrant of α_j and whether the joint axes intersect or are parallel. The remaining DH parameters are straightforwardly found.

For numerical stability, one again wishes to mix the Hayati parameters with the DH parameters for the case of nearly parallel joints. The details that handle all the various cases are presented in Bennett et al. (1992).

5.2. *Jacobian Measurement Method*

Besides CPA, another screw axis measurement method is the *Jacobian measurement method* (Bennett et al. 1992; Hollerbach et al. 1993). The screw Jacobian $\mathbf{J}_s$ matrix for an n-joint manipulator has the form

$$\mathbf{J}_s = \begin{bmatrix} \mathbf{z}_0 & \cdots & \mathbf{z}_{n-1} \\ \mathbf{z}_0 \times \mathbf{b}_1 & \cdots & \mathbf{z}_{n-1} \times \mathbf{b}_n \end{bmatrix}. \tag{61}$$

Thus, the columns of $\mathbf{J}_s$ are the same joint screws (60) as determined by CPA. If one can numerically estimate this Jacobian, then one obtains all of the joint screws at the same time. The Jacobian matrix can be measured in one of two ways:

1. Simultaneous measurement of the end-point force $\mathbf{f}$ and torque $\mathbf{n}$, using a wrist sensor, and of joint torque sensing $\boldsymbol{\tau}$. For a static manipulator, one has the well-known relation

$$\boldsymbol{\tau} = \mathbf{J}_s^T \begin{bmatrix} \mathbf{n} \\ \mathbf{f} \end{bmatrix} + \mathbf{g}, \tag{62}$$

   where $\mathbf{g}$ is the gravity torque vector. The bias of gravity can be eliminated by subtracting a reference exertion. By generating at least six independent wrenches for a 6-DOF manipulator, the relation (62) may be solved for $\mathbf{J}_s$. Interestingly, the manipulator is completely stationary during the calibration.
2. Simultaneous measurement of the end-point linear $\mathbf{v}$ and angular $\boldsymbol{\omega}$ velocity and of the joint angle velocity $\dot{\boldsymbol{\theta}}$ through the well-known relation:

$$\mathbf{J}_s \dot{\boldsymbol{\theta}} = \begin{bmatrix} \boldsymbol{\omega} \\ \mathbf{v} \end{bmatrix}. \tag{63}$$

   By making at least six independent measurements through the same pose, the Jacobian may be estimated.

In Hollerbach et al. (1993), the Jacobian measurement method was implemented on the Sarcos Dextrous Arm by using joint torque sensing and wrist force-torque sensing. At the present time, the results are limited by the accuracies of these sensors. For example, wrist force-torque sensors are known to suffer from cross-coupling effects; a nominal accuracy of 0.5% for on-axis forces and torques can degrade to 3% to 4% for off-axis loading (Hirose and Yoneda 1990). With regard to joint torque sensors, the use of optical sensing may improve future accuracy (Hirose and Yoneda 1989).

With improvements in inertial sensors, the use of end-point velocity sensing could potentially be sufficiently accurate. This method has not yet been implemented.

5.3. *Other Methods*

In Zhuang and Roth (1993) a linear identification method was presented that is neither a kinematic loop method nor a screw axis measurement method, but is listed here because it shares the feature of CPA of moving one joint at a time. The orientation parameters are determined before the displacement parameters. If the orientation parameters are known, the displacement parameters are determined by ordinary least squares since they appear linearly in the forward kinematics. The orientation parameters are determined recursively by moving each joint to two positions, beginning with the base. At each of the two positions, the full end-point pose is measured. A matrix equation is subsequently solved for the orientation parameters for each joint.

In Ma et al. (1994) a procedure was proposed for joint torque sensor calibration, using the arm's own gravity loading and the sinusoidal relation between joint torque and position. As a by-product, the joint angle gains and offsets (2) are also determined. Even after the DH parameters have been determined, the determination of these joint angle parameters must often be repeated because of drifts in the electronics for analog joint sensing. The relation to CPA is in the sense that each joint is moved in a circle one at a time.

6. Conclusions

A taxonomy of kinematic calibration methods has been proposed based on the *calibration index*. All calibration methods are considered as closed-loop methods: for open-loop methods, the measurement system is considered to form a "joint." In such closed loops, some degrees of freedom are sensed (measured components of pose and sensed joint angles), while others are unsensed (unmeasured components of pose, passive end-point constraints, and unsensed joint angles). Measuring a component of pose has the same effect in calibration as constraining a component of pose; the term *kinematic loop method* is therefore proposed to unify open- and closed-loop methods.

The difference between the number of sensed joints and the mobility in such closed loops is termed the *calibration index* and expresses the number of equations per pose available for calibration. Despite the variety of measurement systems and end-point constraints that have been proposed in kinematic calibration, different methods are now nicely comparable in terms of the calibration index. Recent work on multiple-loop mechanisms also fits nicely into this taxonomy. It is also easy to conjure up new calibration methods by choosing a calibration index and different mixes of sensed and unsensed joints.

A synopsis of numerical issues that are critical for accuracy in kinematic calibration was presented. Issues of scaling of task variables and of kinematic parameters were considered at length for purposes of normalization and rank determination. Various performance indices for least-squares analysis were categorized based on how task variables or kinematic parameters were incorporated and scaled, including weighted least squares, and the Gauss-Markov estimate, damped least squares and the minimum variance estimate. The use of singular value decomposition was examined for rank determination and for solution of ill-conditioned least squares problems. Various measures of observability for pose selection were contrasted, and an analogy was made to dexterity measures for redundant robots.

Input noise in the joint angles, seldom considered in the calibration literature, can be significant and is known to lead to bias errors. For the constrained end effector in closed-loop methods, there is essentially no output noise, and the normal procedure for minimizing end-point errors is inappropriate. Total least squares and orthogonal distance regression are methods that handle input noise. An instance in the context of kinematic calibration is the implicit loop method (Wampler et al. 1995), which views all calibration methods as closed-loop methods and places all measurements, whether joint or end-point, on an equal footing.

Screw axis measurement methods identify individual joint axes as lines in space. Kinematic parameters can then be found analytically, without the need for solving a nonlinear optimization problem. Circle point analysis is the major variant of screw axis measurement and proceeds by measuring end-point position during rotation of one joint at a time. It can be viewed as an open-loop method with this particular pose selection. Another variant involves measuring the Jacobian matrix, either with velocity sensing or with joint torque and end-point wrench sensing. Joint angle offsets and gains can also be determined using joint torque sensing, as a side benefit of joint torque sensor calibration using an arm's gravity load

(Ma et al. 1994). It is interesting that measurements from the realm of kinetics can assist in calibration in the realm of kinematics.

Appendix

This appendix demonstrates that input noise causes biases and is adapted from Norton (1986). Consider a system of overdetermined linear equations

$$\mathbf{x}' = \mathbf{C}'\phi,$$

where the parameters ϕ are to be estimated and the true measurements $\mathbf{x}'$ and $\mathbf{C}'$ are both corrupted by noise:

$$\mathbf{x} = \mathbf{x}' + \mathbf{v}, \quad \mathbf{C} = \mathbf{C}' + \mathbf{W},$$

where $\mathbf{x}$ and $\mathbf{C}$ are the actual measurements, and $\mathbf{v}$ and $\mathbf{W}$ are mutually uncorrelated zero-mean noises. The regression equation is

$$\mathbf{x} = \mathbf{C}\phi + \mathbf{e},$$

where the error $\mathbf{e} = \mathbf{v} - \mathbf{W}\phi$ is correlated with the input noise $\mathbf{W}$. The ordinary least squares estimator $\hat{\phi}$ of the true parameters ϕ is

$$\hat{\phi} = (\mathbf{C}^T\mathbf{C})^{-1}\mathbf{C}^T\mathbf{x}.$$

The bias is defined as $\mathbf{b} = \mathbf{E}[\hat{\phi}] - \phi$, where $\mathbf{E}$ is the expectation operator. Substituting for the estimator,

$$\begin{aligned}
\mathbf{b} &= \mathbf{E}[(\mathbf{C}^T\mathbf{C})^{-1}\mathbf{C}^T\mathbf{x}] - \phi \\
&= \mathbf{E}[(\mathbf{C}^T\mathbf{C})^{-1}\mathbf{C}^T(\mathbf{C}\phi + \mathbf{e})] - \phi \\
&= \mathbf{E}[(\mathbf{C}^T\mathbf{C})^{-1}\mathbf{C}^T\mathbf{e}] \\
&= \mathbf{E}[([\mathbf{C}' + \mathbf{W}]^T[\mathbf{C}' + \mathbf{W}])^{-1}[\mathbf{C}' + \mathbf{W}]^T(\mathbf{v} - \mathbf{W}\phi)] \\
&= -\mathbf{E}[([\mathbf{C}' + \mathbf{W}]^T[\mathbf{C}' + \mathbf{W}])^{-1}[\mathbf{C}' + \mathbf{W}]^T\mathbf{W}]\phi.
\end{aligned}$$

This complicated bias assumes a simpler asymptotic form when the number M of measurements increases. The result from Norton (1986) is stated without proof:

$$\mathbf{b} = \text{plim}\left[\frac{1}{M}(\mathbf{C}^T\mathbf{C})^{-1}\right]\mathbf{E}[\mathbf{C}^T\mathbf{e}],$$

where "plim" stands for probability limit.

Acknowledgments

Support for this research was provided by the Natural Sciences and Engineering Research Council (NSERC) Network Centers of Excellence Institute for Robotics and Intelligent Systems (IRIS). Personal support for JMH was provided by the NSERC/Canadian Institute for Advanced Research (CIAR) Industrial Research Chair in Robotics.

References

An, C. H., Atkeson, C. G., and Hollerbach, J. M. 1988. *Model-Based Control of a Robot Manipulator*. Cambridge, MA: MIT Press.

Bennett, D. J., and Hollerbach, J. M. 1988 (Austin, TX, December 7–9) Self-calibration of single-loop, closed kinematic chains formed by dual or redundant manipulators. *Proc. 27th IEEE Conf. Decision and Control*, pp. 627–629.

Bennett, D. J., and Hollerbach, J. M. 1989 (Scottsdale, AZ, May 14–19) Identifying the kinematics of robots and their tasks. *Proc. IEEE Int. Conf. Robotics and Automation*, pp. 580–586.

Bennett, D. J., and Hollerbach, J. M. 1990. Closed-loop kinematic calibration of the Utah-MIT Hand. In Hayward, V., and Khatib, O. (eds.): *Experimental Robotics I — The First International Symposium.*. New York: Springer-Verlag, pp. 539–552.

Bennett, D. J., and Hollerbach, J. M. 1991. Autonomous calibration of single-loop closed kinematic chains formed by manipulators with passive end-point constraints. *IEEE Trans. Robot. Automation* 7:597–606.

Bennett, D. J., Hollerbach, J. M., and Geiger, D. 1990. Autonomous robot calibration for hand-eye coordination. In Miura, H., and Arimoto, S. (eds.): *Robotics Research: the Fifth International Symposium.* Cambridge, MA: MIT Press, pp. 137–144.

Bennett, D. J., Hollerbach, J. M., and Geiger, D. 1991. Autonomous robot calibration for hand-eye coordination. *Int. J. Robot. Res.* 10:550–559.

Bennett, D. J., Hollerbach, J. M., and Henri, P. D. 1992 (Nice, France, May 10–15). Kinematic calibration by direct estimation of the Jacobian matrix. *Proc. IEEE Int. Conf. Robotics and Automation*, pp. 351–357.

Bevington, P. R., and Robinson, D. K. 1992. *Data Reduction and Error Analysis for the Physical Sciences.* New York: McGraw-Hill.

Boggs, P. T., Byrd, R. H., and Schnabel, R. B. 1987. A stable and efficient algorithm for nonlinear orthogonal distance regression. *SIAM J. Sci. Stat. Comput.* 8:1052–1078.

Borm, J. H., and Menq, C. H. 1991. Determination of optimal measurement configurations for robot calibration based on observability measure. *Int. J. Robot. Res.* 10(1):51–63.

Boulet, B. 1992. Modeling and control of a robotic joint with in-parallel redundant actuators. Thesis, Department of Electrical Engineering, McGill University, Montreal, Quebec, Canada.

Bryson, A. E. Jr., and Ho, Y-.C. 1975. *Applied Optimal Control.* Washington, DC: Hemisphere Publishing.

Canepa, G., Hollerbach, J. M., and Boelen, S. 1994 (San Diego, May 8–13). Kinematic calibration by means of

a triaxial accelerometer. *Proc. IEEE Int. Conf. Robotics and Automation*, pp. 2776–2782.

Craig, J. J. 1990 (December). *Silma Manual.* Cupertino, CA:Silma Inc.

Craig, J. J. 1993 (Tokyo, November). Calibration of industrial robots. *Proc. 24th Int. Symp. on Industrial Robots*, pp. 889–893.

Denavit, J., and Hartenberg, R. S. 1955. A kinematic notation for lower pair mechanisms based on matrices. *J. Appl. Mechanics.* 22:215–221.

Doty, K. L., Melchiorri, C., and Bonivento, C. 1993. A theory of generalized inverses applied to robotics. *Int. J. Robot. Res.* 12:1–19.

Driels, M. R. 1993. Using passive end-point motion constraints to calibrate robot manipulators. *J. Dynam. Sys., Meas. Control.* 115:560–565.

Driels, M. R., and Pathre, U. S. 1990. Significance of observation strategy on the design of robot calibration experiments. *J. Robot. Sys.* 7:197–223.

Driels, M. R., and Swayze, W. E. 1994. Automated partial pose measurement system for manipulator calibration experiments. *IEEE Trans. Robot. Automation* 10:430–440.

Fuller, W. A. 1987. *Measurement Error Models.* New York: John Wiley & Sons.

Giugovaz, L., and Hollerbach, J. M. 1994 (Munich, Germany, September 12–16). Closed-loop kinematic calibration of the Sarcos Dextrous Arm. *Proc. IEEE/RSJ Int. Conf. on Intelligent Robots and Systems*, pp. 329–334.

Goswami, A., Quaid, A., and Peshkin, M. 1993a. (Atlanta, May 2–7). Complete parameter identification of a robot from partial pose information. *IEEE Int. Conf. Robotics and Automation*, vol. 1, pp. 168–173.

Goswami, A., Quaid, A., and Peshkin, M. 1993b. Identifying robot parameters using partial pose information. *IEEE Control Sys.* 13(5):6–14.

Hayati, S. A., and Mirmirani, M. 1985. Improving the absolute positioning accuracy of robot manipulators. *J. Robot. Sys.* 2:397–413.

Hirose, S., and Yoneda, K. 1989 (Tokyo, October 4–6). Robotic sensors with photodetecting technology. *Proc. Int. Symp. Industrial Robots*, pp. 271–278.

Hirose, S., and Yoneda, K. 1990 (Cincinnati, May 13–18). Development of optical 6-axial force sensor and its signal calibration considering non-linear interference. *Proc. IEEE Int. Conf. Robotics and Automation*, pp. 46–53.

Hollerbach, J. M. 1989. A review of kinematic calibration. In Khatib, O., Craig, J. J., and Lozano-Pérez, T. (eds.): *The Robotics Review, 1.* Cambridge, MA: MIT Press, pp. 207–242.

Hollerbach, J. M., and Bennett, D. J. 1988. Automatic kinematic calibration using a motion tracking system. In Bolles, R., and Roth, B. (eds.): *Robotics Research: the Fourth International Symposium.* Cambridge, MA: MIT Press, pp. 191–198.

Hollerbach, J. M., and Hunter, I. W. 1990. Robotics: Control without science. *Physics World* (November):17.

Hollerbach, J. M., and Lokhorst, D. 1993 (Atlanta, May 2–7). Closed-loop kinematic calibration of the RSI 6-DOF hand controller. *Proc. IEEE Int. Conf. Robotics and Automation*, vol. 2, pp. 142–148.

Hollerbach, J. M., and Lokhorst, D. 1995. Closed-loop kinematic calibration of the RSI 6-DOF hand controller. *IEEE Trans. Robot. and Automation* 11:352–359.

Hollerbach, J. M., Giugovaz, L., Buehler, M., and Xu, Y. 1993 (Yokohama, Japan, July 26–30). Screw axis measurement for kinematic calibration of the Sarcos Dextrous Arm. *Proc. IEEE/RSJ Int. Conf. on Intelligent Robots and Systems*, pp. 1617–1621.

Khoshzaban, M., Sassani, F., and Lawrence, P. D. 1992. Autonomous kinematic calibration of industrial hydraulic manipulators. In Jamshidi, M., Lumia, R., Mullins, J., and Shahinpoor, M. (eds.): *Robotics and Manufacturing.* New York: ASME Press, pp. 577–584.

Klein, C. A., and Blaho, B. E. 1987. Dexterity measures for the design and control of kinematically redundant manipulators. *Int. J. Robot. Res.* 6(2):72–83.

Lau, K., Hocken, R., and Haynes, L. 1985. Robot performance measurements using automatic laser tracking techniques. *Robot. Computer-Integrated Manufacturing* 2:227–236.

Lawson, C. L., and Hanson, R. J. 1974. *Solving Least Squares Problems.* Englewood Cliffs, NJ: Prentice Hall.

Luenberger, D. G. 1969. *Optimization by Vector Space Methods.* New York: Wiley.

Ma, D., Hollerbach, J. M., and Xu, Y. 1994 (San Diego, May 8–13). Gravity based autonomous calibration for robot manipulators. *Proc. IEEE Int. Conf. Robotics and Automation*, pp. 2763–2768.

Masory, O., Wang, J., and Zhuang, H. 1993 (Atlanta, May 2–7). On the accuracy of a Stewart platform—part II. Kinematic calibration and compensation. *IEEE Int. Conf. Robotics and Automation*, vol. 1, pp. 725–731.

McCarthy, J. M. 1990. *Introduction to Theoretical Kinematics.* Cambridge, MA: MIT Press.

Mooring, B. W., Roth, Z. S., and Driels, M. R. 1991. *Fundamentals of Manipulator Calibration.* New York: Wiley Interscience.

Nahvi, A., Hollerbach, J. M., and Hayward, V. 1994 (San Diego, May 8–13). Closed-loop kinematic calibration

of a parallel-drive shoulder joint. *Proc. IEEE Int. Conf. Robotics and Automation*, pp. 407–412.

Newman, W. S., and Osborn, D. W. 1993 (Atlanta, May 2–7). A new method for kinematic parameter calibration via laser line tracking. *Proc. IEEE Int. Conf. Robotics and Automation*, vol. 2, pp. 160–165.

Norton, J. P. 1986. *An Introduction to Identification.* London: Academic Press.

Press, W. H., Teukolsky, S. A., Vetterling, W. T., and Flannery, B. P. 1992. *Numerical Recipes in C.* Cambridge, UK: Cambridge University Press.

Renders, J.-M., Rossignol, E., Becquet, M., and Hanus, R. 1991. Kinematic calibration and geometrical parameter identification for robots. *IEEE Trans. Robot. and Automation* 7:721–732.

Roth, B. 1984. Screws, motors, and wrenches that cannot be bought in a hardware store. In Brady, M. and Paul, R. (eds.): *Robotics Research: The First International Symposium.* Cambridge, MA: MIT Press, pp. 679–694.

Roth, Z., Mooring, B. W., and Ravani, B. 1987. An overview of robot calibration. *IEEE J. Robot. and Automation.* RA-3:377–386.

Salisbury, J. K., and Craig, J. J. 1982. Articulated hands: Force control and kinematic issues. *Int. J. Robot. Res.* 1(1):4–17.

Schröer, K. 1993. Theory of kinematic modelling and numerical procedures for robot calibration. In Bernhardt, R., and Albright, S. L. (eds.): *Robot Calibration.* London: Chapman & Hall, pp. 157–196.

Schröer, K., Uhl, L., Albright, S., and Huttenhofer, M. 1992 (Tsukuba Science City, Japan, Nov. 16–19). Ensuring solvability and analyzing results of the nonlinear robot calibration problem. *Proc. Second Intl. Symposium on Measurement and Control in Robotics*, pp. 851–858.

Schwetlick, H., and Tiller, V. 1985. Numerical methods for estimating parameters in nonlinear models with errors in variables. *Technometrics* 27:17–24.

Sklar, M. E. 1989 (Boca Raton, FL, May 18–19). Geometric calibration of industrial manipulators by circle point analysis. *Proc. 2nd Conf. on Recent Advances in Robotics*, pp. 178–202.

Sorenson, H. W. 1970. Least-squares estimation: From Gauss to Kalman. *IEEE Spectrum* 7(7):63–68.

Stone, H. W. 1987. *Kinematic Modeling, Identification, and Control of Robotic Manipulators.* Boston: Kluwer Academic.

Tang, G.-R. 1986. Calibration and accuracy analysis of a six-axis industrial robot. Ph.D. thesis, Department of Mechanical Engineering, Texas A&M University.

Tang, G.-R., and Liu, L.-S. 1993. Robot calibration using a single laser displacement meter. *Mechatronics* 3:503–516.

Van Huffel, S., and Vandewalle, J. 1991. *The Total Least Squares Problem: Computational Aspects and Analysis.* Philadelphia: SIAM.

Vincze, M., Prenninger, J. P., and Gander, H. 1994. A laser tracking system to measure position and orientation of robot end effectors under motion. *Int. J. Robot. Res.* 13:305–314.

Wampler, C., and Arai, T. 1992 (Nagoya, Japan, September 24–26). Calibration of robots having kinematic closed loops using non-linear least-squares estimation. *Proc. IFTOMM Symposium* 1:153–158.

Wampler, C. W., Hollerbach, J. M., and Arai, T. 1995. An implicit loop method for kinematic calibration and its application to closed-chain mechanisms. *IEEE Trans. Robot. Automation.* 11:710–724.

Whitney, D. E., Lozinski, C. A., and Rourke, J. M. 1986. Industrial robot forward calibration method and results. *ASME J. Dynam. Sys., Meas. Control* 108:1–8.

Woltring, H. J., Huiskes, R., and De Lange, A. 1985. Finite centroid and helical axis estimation from noisy landmark measurements in the study of human joint kinematics. *J. Biomechanics* 18:379–389.

Yoshikawa, T. 1985. Manipulability of robotic mechanisms. *Int. J. Robot. Res.* 4(2):3–9.

Zak, G., Benhabib, B., Fenton, R. G., and Saban, I. 1994. Application of the weighted least squares parameter estimation method for robot calibration. *J. Mechanical Design* 116:890–893.

Zhuang, H., and Roth, Z. S. 1993. A linear solution to the kinematic parameter identification of robot manipulators. *IEEE Trans. Robot. Automation* 9:174–185.

Zhuang, H., Li, B., Roth, Z. S., and Xie, X. 1992. Self-calibration and mirror center offset elimination of a multi-beam laser tracking system. *Robot. Autonomous Sys.* 9:255–269.

Zhuang, H., Wang, L., and Roth, Z. S. 1993 (Atlanta, May 2–7). Simultaneous calibration of a robot and a hand-mounted camera. *Proc. IEEE Int. Conf. Robotics and Automation*, vol. 2, pp. 149–154.